Fragmentation of Plasma-sprayed Molybdenum Particles on Glass Surfaces

McDonald, A.; Raessi, M.; Chandra, S.; Mostaghimi, J.; Moreau, C.

Publisher's version / la version de l'éditeur:
Proceedings. Thermal Spray 2006: Science, Innovation, and Application, pp. 895-900, 2006

Fragmentation of Plasma-Sprayed Molybdenum Particles on Glass Surfaces

A. McDonald, M. Raessi, S. Chandra, and J. Mostaghimi
Department of Mechanical Engineering, University of Toronto, Toronto, Ontario, Canada

C. Moreau
Industrial Materials Institute, National Research Council Canada, Boucherville, Québec, Canada

Abstract

The impact of plasma-sprayed molybdenum particles on glass surfaces held at 25 and 400°C was photographed. A two-color pyrometer was used to collect thermal radiation from the particles to follow their temperature evolution and to calculate the splat cooling rate. Significant fragmentation of the splat on the surface at 25°C was observed. A 3D model of droplet impact and solidification was used to estimate the thermal contact resistances between the splat and glass. It was found that the thermal contact resistance was approximately two orders of magnitude smaller on the surface at 400°C, indicating faster solidification, which reduced splashing. The larger thermal contact resistance between the non-heated glass and splat was attributed to the presence of a gas barrier at the surface.

Introduction

Fragmentation and splashing of plasma-sprayed particles, after impact, are induced by many factors. Mehdizadeh, et al. [1] have photographed the impact of water droplets impinging on stainless steel surfaces. It was observed that increasing the impact velocity, increased the occurrence of splashing. Li, *et al.* [2] found that application of an organic compound to the substrate surface increased the incidence of splashing. Heating the coated substrate 50 °C above the boiling point of the organic covering, eliminated splashing and produced disk-like splats. Jiang, *et al.* [3] observed that removal of surface contaminants on the substrate, reduced splashing. It was proposed that on non-heated surfaces, these contaminants vaporize and form a gas barrier beneath the splat, restricting splat solidification and promoting fragmentation and splashing of the liquid.

It has been shown that the substrate temperature influences significantly the extent of splashing [4, 5]. Fukumoto, *et al.* [4] have shown that increasing the substrate temperature reduced or eliminated the occurrence of splashing and produced disk-like splats. Fukumoto, *et al.* [4] proposed that the disk-like splats were formed due to good contact between the substrate and splat, increasing the solidification rate of the splat. McDonald, *et al.* [5] showed that the cooling rate of molybdenum splats on heated glass was an order magnitude larger than that on non-heated glass, suggesting that the thermal contact resistance was smaller on heated glass.

The splat fragmentation and splashing observed on non-heated substrates have been attributed to the large thermal contact resistance between this substrate and the splat [6, 7]. Bianchi, *et al.* [6] have used a 1D model to estimate the thermal contact resistance between plasma-sprayed zirconia and stainless steel. It was found that the thermal contact resistance on a non-heated surface may be one to three orders of magnitude larger than that on a heated surface. However, more precise values are needed.

Three-dimensional numerical models have been used to predict the experimentally observed disintegration and splashing patterns during droplet spreading. Pasandideh-Fard, *et al.* [8] used a 3D numerical model to predict the transient splat morphology of molten nickel that impacted a non-heated stainless steel surface. The value of thermal contact resistance used was an order of magnitude estimate.

The objectives of this study were to: (1) to photograph the fragmentation of plasma-sprayed molybdenum particles that impacted glass by using a fast CCD camera; (2) to measure the cooling rates of the splats by two-color pyrometry; and (3) explain the observed splat fragmentation and splashing by estimating the thermal contact resistances between the surfaces and the splat.

Experimental Method

The experimental assembly and method have been described in detail by McDonald, et al. [5] and Mehdizadeh, *et al.* [9]. A schematic diagram of the experimental setup is shown in Figure 1. A SG100 torch (Praxair Surface Technologies, Indianapolis, IN) was used to melt and accelerate the dense,

spherical molybdenum powder particles (SD152, Osram Sylvania Chemical and Metallurgical Products, Towanda, PA), seived to +38 -60 μm. The substrate was a glass microscope slide (Fisher Scientific, Pittsburgh, PA) that was washed with water and ethanol and dried in an oven at 140°C for 30 minutes.

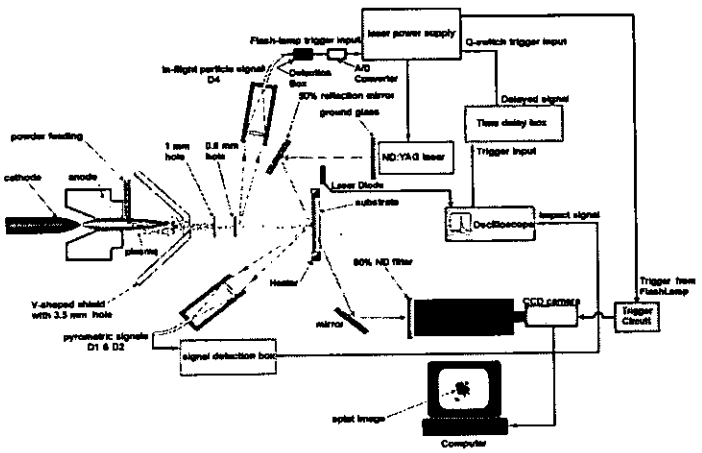

Figure 1: Schematic of the experimental assembly

The thermal radiation of the particle was measured with a rapid two-color pyrometric system. This system included an optical sensor head that consisted of a custom-made lens, which focused the collected radiation, with a 0.21 magnification, on an optical fiber with an 800 μm core [5, 9]. This optical fiber was covered with an optical mask that was opaque to near infrared radiation, except for three slits. The two smaller slits, with dimensions of 30 μm by 150 μm and 30 μm by 300 μm, were used to detect the thermal radiation of the particles in flight. The radiation was used to calculate the temperature, velocity, and diameter of the in-flight particle [7]. The largest slit, measuring 150 μm by 300 μm, was used to collect thermal radiation of the particle as it impacted and spread on the substrate. With the thermal radiation from this slit, the splat temperature, diameter, and cooling rate were calculated at 100 ns intervals after impact.

The thermal emission signals captured by the photodetectors showed the temporal positions of the particle as it passed through the field of view of each of the optical slits. When the particle was not in an optical field of view, the signal voltage was zero. Two small peaks were produced by thermal emissions from the particle as it passed through the first two small slits. The average in-flight velocity of the droplet was calculated by dividing the known distance between the centers of the fields of view of the two slits by the measured time of flight. A plateau on the thermal emission signal corresponded to the presence of the in-flight particle in the field of view of the third and largest optical slit before impact. Upon impact, the signal increased as the particle spread and eventually decreased as the particle cooled down and/or splashed out of the field of view.

To illuminate the impacting particle, a 5±2 ns duration pulse of light from a Nd:YAG laser (Continuum Minilite, Santa Clara, CA) was used. A 12-bit CCD camera (QImaging, Burnaby, BC) was used to capture images of the spreading particles. The camera was connected to a long-range microscope (Astro-optics Division, Montpelier, MD) that had an 80% neutral density (ND) filter to attenuate the intensity of the laser beam. The images captured by the camera were digitized by a frame grabber and recorded on a personal computer. Since the images were not photographed directly, but rather, their reflection in a mirror that was at an angle relative to the substrate, the digitized images were rotated and shortened on both dimensions.

Numerical Method

The three-dimensional numerical model of droplet impact and solidification which is used in this study was developed by Bussmann *et al.* [10] and Pasandideh-Fard *et al.* [11]. Detailed descriptions of the model are found in these references.

The equations of conservation of mass and momentum governing the liquid phase in the presence of a solid phase are

$$\vec{\nabla}\cdot(\Theta\vec{V}) = 0\,; \qquad (1)$$

$$\frac{\partial(\Theta\vec{V})}{\partial t} + (\Theta\vec{V}\cdot\vec{\nabla})\vec{V} = \frac{-\Theta}{\rho}\vec{\nabla}p + \Theta\upsilon\nabla^2\vec{V} + \frac{\Theta}{\rho}\vec{F_b}\,, \qquad (2)$$

where $\vec{V}$ represents the velocity vector, p the pressure, ρ the density, υ the kinematic viscosity, and $\vec{F_b}$ any body forces acting on the fluid. In these equations, Θ denotes the liquid-solid fraction, which is equal to one when the material is in the liquid phase and zero in the solid phase. The free surface of the liquid is defined by using the "Volume of Fluid" (VOF) method, in which a scalar function, f, is set equal to one in the droplet material (liquid or solid) and set equal to zero outside. Since f is passively advected with the flow, it satisfies the advection equation, which, in the presence of the solid phase, is

$$\frac{\partial f}{\partial t} + (\Theta\vec{V}\cdot\vec{\nabla})f = 0\,. \qquad (3)$$

The energy equation, which is solved for heat transfer and phase change, is [11]

$$\rho\frac{\partial h}{\partial t} + \rho(\vec{V}\cdot\vec{\nabla})h = \vec{\nabla}\cdot(k\vec{\nabla}T)\,, \qquad (4)$$

where h represents the enthalpy, k the conductivity, and T the temperature. To solve the energy equation, the enthalpy transforming model [12] is used to convert the energy equation to one with enthalpy as the single dependent variable. This method represents the energy equation for both phases simultaneously.

These governing equations were solved using a finite volume technique on a three-dimensional Cartesian structured grid. Since symmetry boundaries were utilized to reduce the problem size and to save computational time, only one-quarter of the droplet and splat were modelled. Along the symmetry boundaries, the fluid flow obeys free slip and no-penetration conditions and an adiabatic thermal boundary condition was applied. Numerical computations were performed on an AMD Athlon 64, 3400 PC. The average CPU time was 24 hours.

Results and Discussion

Images and Thermal Emission Signals

McDonald, *et al.* [5] and Mehdizadeh, *et al.* [9] have photographed the impact and spreading of molybdenum particles on glass held at room temperature and at 400 °C. Figures 2 and 3 show summaries of the images and thermal emission signals of the particles on heated and non-heated glass, respectively. The average particle in-flight velocity was 135 m/s and the temperature in flight was 2976 °C.

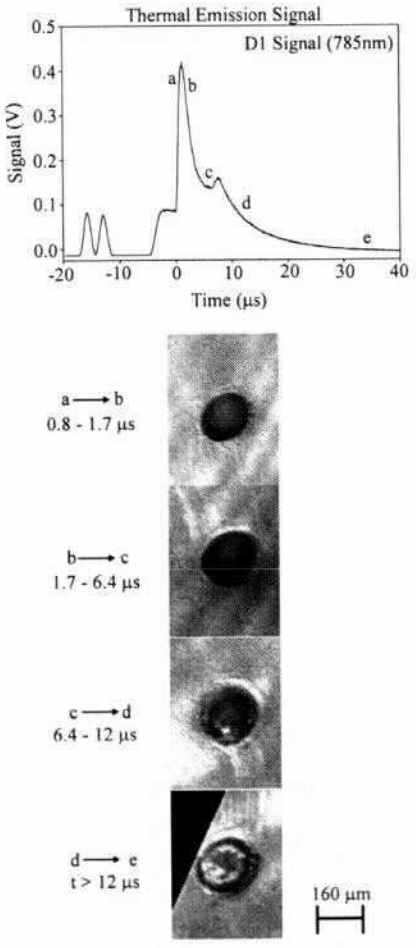

Figure 2: A typical thermal emission signal and images of molybdenum splats at different times after impact on glass held at room temperature

Figure 2 shows that on the heated glass, fragmentation and splashing of the splat is significantly reduced compared to on non-heated glass (Fig. 3). After achieving the maximum spread diameter (~140 μm), as shown in sequence *a* to *b* of figure 2, the splats on heated glass fragmented near their periphery (see sequence *d* to *e* of Fig. 2). On glass held at room temperature (Fig. 3), perforations in the thin film grew as the splat fragmented and splashed, leaving only a solidified central core. Sequence *f* to *g* of figure 3 shows that the splat achieved the maximum spread diameter (~400 μm) just before the rest of the splat detached from the solidified central core (sequence *g* to *h* of figure 3).

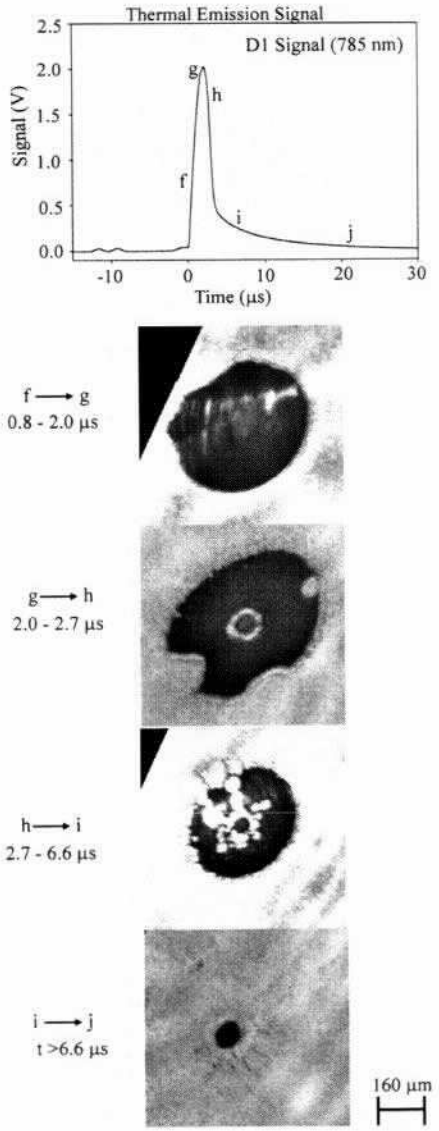

Figure 3: A typical thermal emission signal and images of molybdenum splats at different times after impact on glass held at ~400 °C

Occurrence of Splashing

Moreau, *et al.* [13] have shown that, on a typical thermal emission signal for the impact of molybdenum on non-heated surfaces, there is a transition from a period of relatively high voltage decrease, immediately after achieving the maximum diameter, to a period of slow voltage decrease. This slow voltage decrease indicates that material splashes and exits the pyrometric field of view as explained below.

Figure 4 shows a typical thermal emission signal for a molybdenum splat on a non-heated surface with two fields of view. In order to determine when splashing occurs, two fields of view, of different sizes, were focused at the impact point on the substrate. The larger field of view, D_3, had an area of 4.5 mm^2, while the smaller, D_1, had an area of 0.5 mm^2. The radiation collected in both fields of views were at the same wavelength. The thermal emission signals from the two fields of view were similar, until ~3 μs after impact, when the voltage signal from the larger field of view (D_3) was larger than that from the smaller field of view (D_1), indicating that thermal radiation from the splat was lower in the D_1 field of view. This suggested that material exited the D_1 field of view, due to splashing, 3 μs after impact of the particle. The *g* to *h* and *h* to *i* sequences of figure 3 show that splat fragmentation changes to splat splashing approximately 3 μs after particle impact.

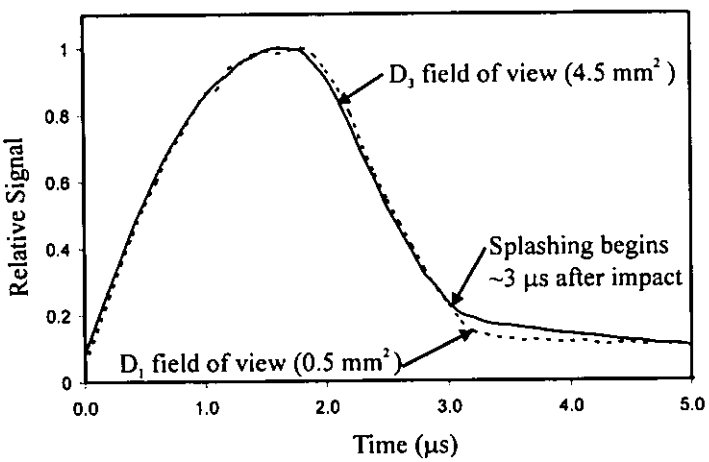

Figure 4: Superimposed thermal emission signals of a molybdenum splat showing splash initiation

Temperature Evolution

Curves depicting the temperature evolution of plasma-sprayed molybdenum on heated and non-heated surfaces have been shown by McDonald, *et al.* [5]. The cooling rate $\left(\frac{dT}{dt}\right)$ of the splat was calculated from the temperature at the maximum extent to either the solidification plateau, in the case of the splats on glass held at 400 °C, or to the point where splashing began on the non-heated surface (~3 μs after particle impact). On heated glass, the cooling rate was an order of magnitude larger (2.1 x 10^8 K/s) than that on non-heated glass (4.8 x 10^7 K/s). Fukumoto, *et al.* [4] have proposed that on the heated surface, the contact between the splat and substrate is better than that on a non-heated surface. This suggests that the thermal contact resistance between the heated surface and the splat was smaller.

Numerical Results

A 3D numerical model of droplet impact and solidification was used to estimate the values of the thermal contact resistance, in addition to simulating the spreading and fragmentation of the splat observed in figures 2 and 3. Figure 5a shows the simulated images of a 45 μm diameter molybdenum droplet, initially at 2990°C, impinging glass held at 400°C, with an impact velocity of 145 m/s. The thermal contact resistance was set to 3.0 x 10^{-7} m^2K/W. To show the extent of solidification in the computer generated images, the liquid was made transparent, with a light gray color. Solid layers were assigned a darker shade of gray. The simulated images show that 0.84 μs after impact, fragmentation of the liquid is due to locally solidified areas in the spreading droplet, which breaks the thin liquid film at its periphery (Fig. 5a). This morphology agrees with that observed in sequence *d* to *e* of figure 2. The maximum spread diameter, as measured from the image at 0.8 μs after impact (Fig. 5a), is ~200 μm. The experimental maximum spread diameter was ~140 μm. The predicted maximum spread diameter is probably larger due to the larger in-flight diameter (45 μm) and in-flight velocity (145 m/s) used in the simulations, compared to the experimental mean particle diameter (40 μm) and mean in-flight velocity (135 m/s). The particle diameter is about 15% larger in the simulation and the impact velocity is about 10% larger. These differences probably contributed to a maximum spread diameter that was about 40% larger in the simulations, compared to that observed in the experiments.

Figure 5b shows the same molybdenum particle, impacting glass held at 400 °C, but with a thermal contact resistance of 2.5 x 10^{-7} m^2K/W. This small decrease of the thermal contact resistance, from 3.0 x 10^{-7} m^2K/W to 2.5 x 10^{-7} m^2K/W, eliminates the splat fragmentation observed in the images of figure 5a. This is probably attributed to an increased heat transfer rate, which enhances solidification before liquid fragmentation.

Figure 6 shows the impact of a 50 μm diameter molybdenum droplet, impinging at 150 m/s onto a glass substrate initially at 27 °C. The droplet initial temperature is 3050 °C. Similar to figure 5a, the liquid was made partially transparent. To simulate the effect of a gas barrier beneath the splat, as proposed by Jiang, *et al.* [3], a slip boundary condition was implemented at the substrate surface. Since the cooling rate was an order of magnitude lower on the non-heated glass, it was assumed that a gas barrier restricted heat transfer [3]. The liquid splat slipped over this barrier as it spread on the glass surface. The images of figure 3 show that only a solidified

core remains on the surface, long after impact. Gougeon and Moreau [14] have measured the size evolution of molybdenum splats on glass at room temperature by using high-speed two-color pyrometry. It was found that the solid core that remains on the substrate after the rest of the splat have splashed away is ~$1.5D_o$.

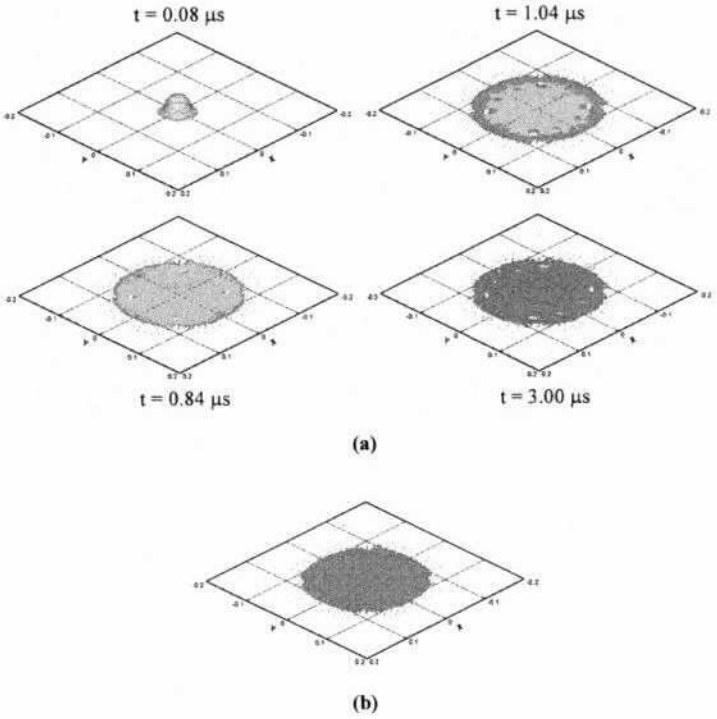

Figure 5: Computer generated images of (a) 45 μm diameter molybdenum droplet initially at 2990 °C impacting with velocity of 145 m/s onto glass initially at 400 °C with contact resistance of 3.0 x 10^{-7} m^2K/W and (b) same conditions as above, but with thermal contact resistance of 2.5 x 10^{-7} m^2K/W. Each square represents 100 μm

This solidified core was probably formed as a result of good contact with the substrate due to the high pressure beneath the splat at the time of impact [9], while the rest of the fluid flowed and slipped over the gas barrier [3]. As a result, the thermal contact resistance in the simulations on the non-heated surface will be spatially varying. The thermal contact resistance in a circular area, centered at the impact point and with a radius 1.5 times the droplet radius, was set to 1.0 x 10^{-7} m^2K/W, to simulate the improved contact between the central core fluid and the substrate surface. In this core region, it was assumed that a no-slip boundary condition existed at the liquid splat-substrate interface. Outside this region, the contact resistance was set to 3.4 x 10^{-5} m^2K/W, two orders of magnitude larger than on glass held at 400 °C. In this region of the splat, a slip boundary condition was applied at the splat-substrate interface to model flow over the gas barrier. The images of figure 6 show that as the splat spreads on the substrate, the liquid film detaches from the solidified, central core, about 1.13 μs after impact. The maximum spread diameter, as predicted by the model in the image at 1.13 μs after impact (Fig. 6), is ~400 μm. This agrees well with the experimental observations of figure 3 (~400 μm). The disintegration pattern, as predicted by the the simulation, agrees partially with the experimental results. The simulations predict that a solidified, central core remains on the surface after disintegration and splashing. However, it fails to predict that before splashing occurs, the splat breaks due to the formation of holes in the thin, liquid film. A two-fluid model, capable of simulating the gas barrier between the splat and substrate, may predict better the observed disintegration pattern.

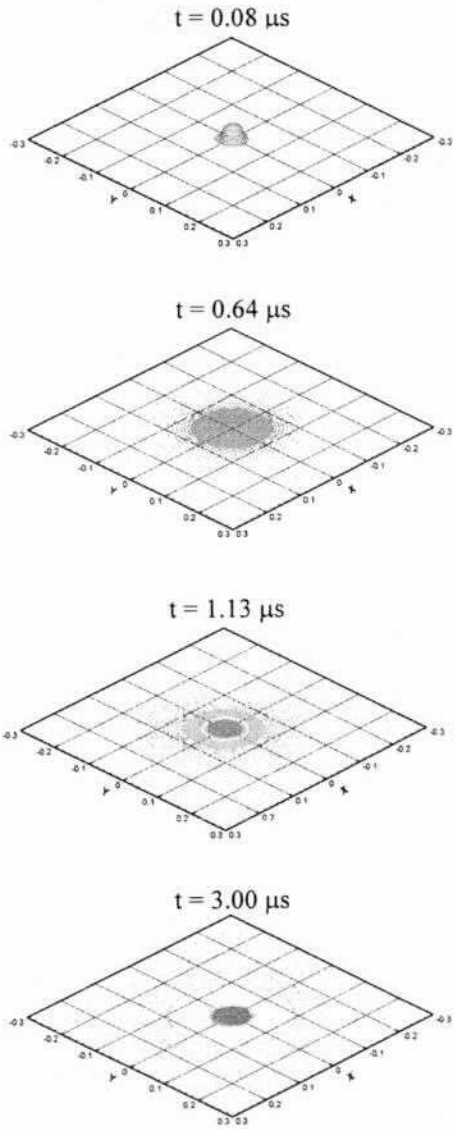

Figure 6: Computer generated images of a 50 μm diameter droplet at 3050 °C, impinging at 150 m/s onto a glass substrate initially at 27 °C, with spatially varying thermal contact resistance. Each square represents 100 μm

The order of magnitude difference in the thermal contact resistances confirm the experimental observations of figures 2 and 3. On heated glass, where the thermal contact resistance is smaller, the splat solidifies faster, reducing the occurrence of splashing and producing a smaller maximum diameter (~140 μm), compared to on non-heated glass (~400 μm). On non-heated glass, the splat remains as a liquid longer, due to the lower rate of heat transfer to the substrate, and eventually fragments and splashes. Jiang, *et al.* [3] have proposed that on a non-heated surface, the vaporization of adsorbates and condensates on the surface forms a gas barrier beneath the splat. Heating the surface, removes the adsorbates and condensates and eliminates the gas barrier. Fukumoto, *et al.* [4] have suggested that this gas barrier, which is absent on a heated surface, restricts heat transfer from the splat to the substrate.

Conclusion

The fragmentation and splashing of plasma-sprayed molybdenum on heated and non-heated glass were studied. On non-heated glass, the splat fragmented and eventually splashed off the surface, leaving only a solidified central core. The degree of fragmentation and splashing was less in the splat on heated glass, with only fragmentation at the periphery. The maximum spread diameter of the splats on non-heated glass was approximately two times larger than those on heated glass. The cooling rate, as calculated from 2-color pyrometric signals, of splats that impacted heated glass was an order of magnitude larger to non-heated glass, suggesting that the thermal contact resistance was lower.

A 3D numerical model of droplet impact and solidification was used to estimate the thermal contact resistances. It was found that on the heated glass, the thermal contact resistance was two orders of magnitude lower than that on non-heated glass. This was attributed to the presence of a gas barrier between the splat and the non-heated substrate, which restricted heat transfer. The maximum spread diameters predicted by the numerical model agreed with experimental observations. The fragmentation pattern on the heated glass, as predicted by the model, also agreed with the experimental images. A two-fluid numerical model, capable of modelling flow over the gas barrier between the splat and the non-heated glass, may provide better agreement between the numerical and experimental splat disintegration patterns.

References

1. N. Mehdizadeh, S. Chandra, and J. Mostaghimi, Formation of fingers around the edges of a drop hitting a metal plate with high velocity, *J. Fluid Mech.*, Vol 510, 2004, p. 353 – 373
2. C. Li, J. Li, and W. Wong, The effect of substrate preheating and surface organic covering on splat formation, *Thermal Spray: Meeting the Challenges of the 21st Century*, C. Coddet, Ed., May 25-29, 1998 (Nice, France), ASM International, 1998, p. 473 – 480
3. X. Jiang, Y. Wan, H. Hermann, S. Sampath, Role of Condensates and Adsorbates on Substrate Surface on Fragmentation of Impinging Molten Droplets During Thermal Spray, *Thin Solid Films*, Vol 385, 2001, p. 132 – 141
4. M. Fukumoto, E. Nishioka, and T. Matsubara, Flattening and solidification behavior of a metal droplet on a flat substrate surface held at various temperatures, *Surface Coatings and Technology*, Vol 120 – 121, 1999, p. 131 – 137
5. A. McDonald, M. Lamontagne, C. Moreau, and S. Chandra, Visualization of impact of plasma-sprayed molybdenum particles on hot and cold glass substrates, *International Thermal Spray Conference 2005*, Plasma Spraying, E. Lugscheider, Ed., May 2-4, 2005 (Basel, Switzerland), ASM International, 2005, p. 1192 – 1197.
6. L. Bianchi, A. Leger, M. Vardelle, A. Vardelle, and P. Fauchais, Splat formation and cooling of plasma-sprayed zirconia, *Thin Solid Films*, Vol 305, 1997, p. 35 – 47
7. C. Moreau, P. Cielo, M. Lamontagne, S. Dallaire, M. Vardelle, "Impacting particle temperature monitoring during plasma spray deposition", *Meas. Sci. Technol.*, Vol 1, 1990, p. 807 – 814
8. M. Pasandideh-Fard, V. Pershin, S. Chandra, and J. Mostaghimi, Splat shapes in a thermal spray coating process: Simulations and experiments, *J. of Thermal Spray Tech.*, Vol 11 (No. 2), 2002, p. 206 – 217
9. N. Mehdizadeh, M. Lamontagne, C. Moreau, and S. Chandra, Photographing impact of molten molybdenum particles in a plasma spray, *J. Thermal Spray Tech.*, Vol. 14, 2005, p. 354 - 361
10. M. Bussmann, J. Mostaghimi, and S. Chandra, On a three-dimensional volume tracking model of droplet impact, *Physics of Fluids*, Vol 11, 1999, p. 1406-1417.
11. M. Pasandideh-Fard, S. Chandra, and J. Mostaghimi, A three-dimensional model of droplet impact and solidification, *Int. J. Heat Mass Transfer*, Vol 45, 2002, p. 2229-2242.
12. Cao, A. Faghri, and W. S. Chang, A Numerical Analysis of Stefan Problems for Generalized Multi-dimensional Phase-Change Structures Using the Enthalpy Transforming Model, *Int. J. Heat Mass Transfer*, Vol. 32 (No. 7), 1989, p. 1289–1298
13. C. Moreau, P. Gougeon, and M. Lamontagne, Influence of substrate preparation on the flattening and cooling of plasma-sprayed particles, *J. Thermal Spray Tech.*, Vol 4 (No. 1), 1995, p. 25 – 33
14. P. Gougeon and C. Moreau, "Simultaneous independent measurement of splat diameter and cooling time during impact on a substrate of plasma-sprayed molybdenum particles", *J. of Thermal Spray Tech.*, Vol 10 (No. 1), 2001, p. 76 – 82